PATENT

IN THE UNITED STATES PATENT AND TRADEMARK OFFICE

In re Application of:	)	Group Art Unit: 1642
	)	
Gregory J. Riggins *et al.*	)	Examiner: C. Yaen
	)	
Serial No.: 09/853,880	)	Atty. Docket No. 000250.00003
	)	
Filed: May 14, 2001	)	

For: FOUR GENETIC TUMOR MARKERS SPECIFIC FOR HUMAN GLIOBLASTOMA

DECLARATION OF GREGORY J. RIGGINS UNDER 37 C.F.R. § 1.132

U.S. Patent and Trademark Office
Customer Service Window, Mail Stop Amendment
Randolph Building
401 Dulany Street
Alexandria, VA 22314

I, Gregory J. Riggins, declare as follows:

1. I am named as an inventor of the subject matter of application Serial No. 09/853,880. In our efforts to identify novel glioma-associated antigens, my colleagues and I previously reported several genes that are preferentially expressed in Glioblastoma Multiforme (GBM) by the serial analysis of gene expression method (13; numbered references are listed in Exhibit 6). Among these candidate GBM marker genes, glycoprotein nmb (GPNMB) showed a greater than 10-fold induction of mRNA expression over normal brain samples in 5/12 of GBM cases (13).

2. In the work I describe below, we performed genetic and immunohistochemical evaluation of human gliomas to determine the incidence, distribution, and pattern of localization of GPNMB antigens in brain tumors. In order to evaluate the therapeutic potential of GPNMB as a GBM-associated antigen, a series of 50 newly diagnosed GBM biopsy specimens were examined for GPNMB RNA transcript levels by real-time reverse transcription-polymerase chain reaction (RT-PCR). In addition, a larger panel of 79 newly diagnosed GBM cases, including 39 out of the 50 samples in the mRNA study, was assessed for GPNMB protein expression by immunohistochemical analysis, and survival analyses were performed based on these two parameters. We demonstrated that significant numbers of GBMs overexpress GPNMB at the mRNA and protein levels, and that expression levels correlate with poorer prognosis for those patients. We conclude that therapeutic strategies designed to target GPNMB may be successful in the treatment of malignant glioma.

3. GPNMB is a type I transmembrane protein which was isolated from a subtractive cDNA library based on differential expression between human melanoma cell lines with low and high metastatic potential in nude mice. GPNMB mRNA was expressed at high levels in low-metastatic melanoma cell lines and xenografts (14). The human GPNMB gene encodes a predicted 560-amino acid protein, the deduced amino acid sequence of which shows that GPNMB is made up of three domains: a long extracellular domain (ECD) preceded by a signal peptide, a single transmembrane region, and a relatively short cytoplasmic domain. See Exhibit 1, which is a schematic protein domain structure of human GPNMB and its alternatively spliced variant insertion in glioblastoma-derived cell lines. Additional description of Exhibit 1 is provided in Exhibit 10.

4. The human GPNMB amino acid sequence has homology of 71.1% to DC-HIL (15), 69.8% to Osteoactivin (16), 56% to the precursor of pMel 17 (17), and 51% to QNR-71 (18). The human GPNMB gene is localized to human chromosome 7q15 (NCBI Unigene Cluster Hs.82226 GPNMB), a locus involved in the human inherited disease cystoid macular dystrophy. Recently, Bachner *et al.* suggested that human GPNMB may be a candidate gene for the dominant cystoid macular edema b they found high expression of murine GPNMB mRNA within the retinal and iris pigment epithelium (19).

5. The function of GPNMB has not been fully described, and paradoxical effects have been noted in transfection studies. Transfection of our *in vitro* minimally transformed human fetal astrocyte line THRG (20) with GPNMB cDNA altered the phenotype of both subcutaneous and intracranial tumors growing in athymic mice from a minimally invasive to a highly invasive and metastatic phenotype. Conversely, transfection of a partial GPNMB cDNA into a highly metastatic melanoma cell line resulted in slower subcutaneous tumor growth and also in reduction of the potential for spontaneous metastasis in nude mice (14).

6. If the overexpression of GPNMB RNA by gliomas and lack of expression in normal brain is reflective of GPNMB protein expression, GPNMB, as an integral membrane protein, could be an important target for immunotherapy. Moreover, there is evidence that GPNMB may be involved in the invasive malignant phenotype of gliomas, making evaluation of GPNMB-expressing cells important (21). In our previous analysis, we could not detect GPNMB transcripts in four normal brain cortex samples, two whole brain samples, or one sample each of cerebellum, spinal cord, heart, kidney, lung, trachea, tonsil, or bone marrow (13). Therefore, in

the work described below, we investigated the suitability of this GPNMB marker as a glioma therapeutic target.

Cell Lines, Cell Transfection, and Tumor Xenografts

7. Human malignant glioma (MG)-derived cell lines D54 MG, D245 MG, D247 MG, and D392 MG were established and maintained in our laboratory; the glioma cell lines U87 MG, T98G (MG), U251 MG, and the melanoma (MEL) cell lines SK-Mel-28, A375, C32, and Malme-3M were obtained from the ATCC (Manassas, VA). MG and MEL cell lines were grown in Zinc Option medium supplemented with 10% FCS (ZO-10% FCS); the propagation, storage, and testing of these cell lines to ensure the absence of HeLa cell contamination, inter- or intra-cell line contamination, or Mycoplasma infection have been published previously (22). The THRG cell line (20, 21), a genetically defined human fetal astrocyte line transfected to express GPNMB, was used as the positive control cell line for GPNMB expression. Human malignant glioma xenogafts D256 MGX, D270 MGX, D320 MGX, D456 MGX, D2159 MGX were established and maintained in our laboratory; the malignant glioma xenografts 6B4-7 and 12A-7 were obtained from Dr. David James (Mayo Clinic, Minnesota).

8. For transient expression experiments, the ECD of *gpnmb* (nucleotides 1-1458, adenosine of the start codon as 1) was ligated into the mammalian expression vector pcDNA3.1 (Invitrogen, Carlsbad, CA). The resulting pcDNA3.1- *gpnmb* $_{ECD}$ was introduced into HEK293 cells by using the Lipofectamine 2000 reagent (Invitrogen, Carlsbad, CA), and transiently transfected cells were harvested 48 hours later. To generate stable GPNMB-transformants, the EcoRI-XhoI fragment of the pWD77 vector containing the full-length *gpnmb* cDNA (obtained from H. P. Bloemers, University Nijjmegen, The Netherlands) (14) was cloned into the retroviral

vector pBabeBleo or pBabeNeo (23). The glioma cell lines D247 MG, D54 MG, and U251 MG were infected with retrovirus as described previously (21), and stably transfected clones were selected in medium containing 200 μg/ml of Zeocin (Invitrogen, Carlsbad, CA) or 1 mg/ml Geneticin (Gibco, Carlsbad, CA).

cDNA Cloning of *gpnmb* from Glioma Cells

9. For cDNA cloning of the *gpnmb* gene from human glioma cells, mRNA was isolated from D392 MG cells using the FastTrack 2.0 Kit (Invitrogen, Carlsbad, CA). After cDNA synthesis using random primers and SuperScript II RNaseH$^-$ Reverse Transcriptase (Life Technologies, Rockville, MD), the DNA fragment encoding the ECD of GPNMB was amplified by one cycle of 95°C for 2 minutes followed by 30 cycles of 94°C for 30 seconds, 60°C for 30 seconds, and 72°C for 1 minute with the following primers:

$GPNMB_{ECD\ FWD}$ (sense): 5′-ATGGAATGTCTCTACTAT-3′

$GPNMB_{ECD\ REV}$ (anti-sense): 5′-GTTTGCCATCCTTAAAGG-3′.

10. The PCR products were further subcloned into pCR2.1TOPO vector (Invitrogen, Carlsbad, CA) and sequenced on both strands using ABI377 automatic sequencer (Applied Biosystems, Foster City, CA).

Quantitative Real-Time RT-PCR Assay

11. Total RNA was isolated from subconfluent cultured cells and sample tissues using the RNeasy Mini Kit (Qiagen, Valencia, CA), and then treated with RNase-free-DNase I (Ambion, Austin, TX). Total RNA sample of normal adult whole brain was purchased from Clontech (Palo Alto, CA). Total RNA (0.2 μg) was converted to cDNA with random primers and SuperScript II RNaseH$^-$ Reverse Transcriptase (Life Technologies, Rockville, MD) in a reaction

volume of 20 µl. After the first-strand cDNA synthesis, 280 µl of water was added to the reaction mixture, and 2 µl of diluted cDNA sample was subjected to real-time PCR measurements.

12. DNA sequencing of RT-PCR products revealed an alternative splicing of *gpnmb* RNA transcripts in human glioma cells (see Exhibit 1). To determine the expression levels of each *gpnmb* RNA transcript relative to that of *β-actin*, the following primers were used in real-time PCR:

GPNMB A (sense) 5′-CACTTCCTCAATTATTCTAC-3′

GPNMB B1 (antisense) 5′-TAAAGAAGGGGTGGGTTTTG-3′

GPNMB B2 (antisense) 5′-TTGTCACCAGCAGGTCCTAA-3′

GPNMB B3 (antisense) 5′-TGGGGTGTTTGAATCATAAG-3′

β-actin$_{FWD}$ (sense) 5′-CCAACCGCGAGAAGATGACCCAGATCATGT-3′

β-actin$_{REV}$ (antisense) 5′-GTGAGGATCTTCATGAGGTAGTCAGTCAGG-3′

13. Primer B1, paired with primer A, amplified the overall *gpnmb* mRNA (both of the wild-type and the spliced variant), while primer B2 was located spanning the exon-exon junction to detect only the wild-type *gpnmb* transcripts (*GPNMB*$_{wt}$). Primer B3, complimentary to the insert sequence generated by alternative splicing, was specific to the splice variant form of *gpnmb* mRNA (*gpnmb*$_{sv}$). Exhibits 2A and 2B show expression of *gpnmb* RNA in glioblastoma and melanoma cell lines and glioma xenografts.

14. *β-actin* transcript was amplified simultaneously as an internal control in each sample. For the PCR reactions, 2 µl of cDNA, 5 µl of 2X SYBR Green PCR Master Mix (Applied Biosystems, Warrington, U.K.), and 400 nM of each primer were used in a total volume

of 10 μl. Cycling parameters were 50°C for 2 minutes and 95°C for 10 minutes, followed by 40 cycles (45 cycles for the detection of splice variant, $gpnmb_{SV}$) of 95°C for 15 seconds and 58°C for 30 seconds. Incorporation of SYBR Green dye into the PCR products was monitored with an ABI PRISM 7900HT Sequence Detector System (Applied Biosystems, Foster City, CA). Integrity of PCR products was confirmed by dissociation curve analysis (SDS 2.0 software, Applied Biosystems, Foster City, CA) and by an agarose gel electrophoresis. To normalize the degradation of total RNA used in cDNA synthesis, the threshold cycle (CT) values were determined for *gpnmb* and corresponding *β-actin* genes in each sample, and the *gpnmb /β-actin* ratio was calculated from the following formula (24):

$$gpnmb\ /\beta\text{-}actin \text{ ratio} = 2^{(C_T\ \beta\text{-actin} - C_T\ \text{GPNMB})}.$$

15. Relative *gpnmb* mRNA levels were expressed in terms of fold induction rate over control normal whole brain sample, which was determined by dividing *gpnmb /β-actin* ratio of tumor sample by that of normal whole brain. All measurements were performed in triplicate, and the experiments were repeated twice.

Recombinant Protein Preparation and Exoglycosidase Treatment

16. The extracellular domain (ECD) of GPNMB protein, $GPNMB_{ECD}$, was produced with a hexahistidine tag at the carboxy-terminus. The extracellular segment of *gpnmb* (nucleotides 64-1458) excluding the signal peptide region was cloned into a T7-based prokaryotic expression vector (25). $GPNMB_{ECD}$ was expressed in *Escherichia coli* BL21-CodonPlus (DE3) RIL (Stratagene, La Jolla, CA) as inclusion bodies. After dissolution in a buffer containing guanidine, $GPNMB_{ECD}$ was purified with an Ni-NTA column (Qiagen, Valencia, CA) and renatured as described previously (26).

17. To produce $GPNMB_{ECD}$ protein in the baculovirus system, the same DNA fragment was fused with baculoviral vector pVL1393 (BD Pharmingen, San Diego, CA). After infecting High Five insect cells with high titer viral stock, GPNMB protein was purified from culture supernatant using Ni-NTA column according to manufacturer's instructions.

18. For exoglycosidase digestion, total cell lysates of 20 μg of protein were denatured by boiling at 100°C for 10 minutes with 0.5% SDS, and then incubated with 10,000 units/ml of Peptide *N*-Glycosidase F (PNGaseF) (New England Biolab, Beverly, MA) in the presence of 1% Nonidet P 40 at 37°C for 2 hours. Samples were subjected to SDS-PAGE and immunoblotting to determine change in molecular mass.

Immunization

19. Immunization protocols utilized an initial DNA immunization with the plasmid vectors encoding the ECD of GPNMB, followed by boosting with the corresponding recombinant protein produced in bacteria. Rabbits were given a primary subcutaneous (s.c.) immunization with 250 μg of mammalian expression vector pcDNA3.1- $gpnmb_{ECD}$ or were immunized with 250 μg of bacterial recombinant $GPNMB_{ECD}$ protein emulsified 1:1 in Freund's Complete adjuvant (CFA); this was followed by 2 times of boosts with 250 μg of $GPNMB_{ECD}$ protein + Freund's incomplete adjuvant (IFA) at 4-week intervals. Rabbits were bled 12 days after the last boost. Titers in serum were monitored by ELISA with $GPNMB_{ECD}$ as the capture antigen and live-cell ELISA using *gpnmb*-expressing D54 MG cells as targets.

20. For mice, the first immunization protocol (referred to as "B") was a combination protocol using pDNA for initial immunizations, followed by purified, bacterially expressed GPNMB protein later in the immunization protocol, since titers insufficient for fusion were

obtained after pDNA immunization alone. On days 1, 49, and 77, Balb/c, C3H/He, and C57Bl/6 mice received 15 μg of GPNMB encoding pDNA in 100 μl intradermally (i.d.); 50% end-point titers vs. GPNMB protein determined with serum obtained on day 89 were less than 1/1000. The mice then received 30 μg of GPNMB protein + CFA on day 156 and a similar boost in IFA on day 176. The 50% end-point serum titers vs. source of GPNMB determined on day 188 were in excess of 1/5000. Following a minimum interval of 30 days, Balb/c recipients were boosted intraperitoneally (i.p.) with 5 μg of protein, and spleens were harvested for fusion 3 to 4 days later. From the fusion using protocol B, MAb G11 was obtained. The second immunization protocol (U) consisted solely of protein immunization: day 1, 30 μg of GPNMB + CFA; days 21, 42, and 63, 15 μg protein + IFA. The 50% end-point serum titers obtained on day 74 were in excess of 1/10,000. On day 105, C57Bl/6 recipients were boosted and spleens harvested as described above; the anti-GPNMB U2 MAb was derived from this fusion.

Fusion, Isolation, and Screening of GPNMB Reactive MAbs

21. Fusions were performed with the non-immunoglobulin-secreting Kearney variant of P3X63/Ag8.653 by using our standard procedure (27). Supernatants were screened for positivity on the bacterially derived GPNMB protein by ELISA and on THRG cells by FMAT assay (see below). Hybridoma supernatant reactivity for plated protein was performed as previously published (27), with the exception that the secondary reagent used was goat anti-mouse IgG-Fc specific (Sigma, St. Louis, MO); the tertiary reagent was horseradish peroxidase (HRP)-Streptavidin (Zymed; South San Francisco, CA); and development was by the SigmaFast o-phenylenediamine dihdrochloride kit (Sigma) according to manufacturer's instructions.

Fluorometric Microvolume Assay Technology (FMAT) Analysis

22. Analysis of MAb binding (supernatant samples or purified MAbs) to intact cell surfaces was performed on the FMAT 8100 HTS system (Applied Biosystems, Foster City, CA). THRG cells grown in 10%FCS-ZO were harvested and fixed with 10% formaldehyde/PBS for 6 minutes at room temperature, then plated into an FMAT 96-well plate at a concentration of 10,000 cells/well; 30 µl of purified anti-GPNMB MAbs or hybridoma supernatants was added to the wells; the positive primary antibody control was the serum pool derived from immunized spleen donors, and negative background controls included 10%FCS-ZO (hybridoma supernatant control), 1% BSA/PBS buffer, or irrelevant isotype controls (IgG_1 or IgG_{2b}) at identical concentrations to the primary reagents. Secondary antibody goat anti-mouse IgG (Jackson ImmunoResearch Laboratories, West Grove, PA) coupled to FMAT-blue dye according to manufacturer's instructions (Applied Biosystems, Foster City, CA) was added to the wells at a final concentration of 0.13 µg/ml in 1%BSA/PBS, and the plates were incubated for 2 hours in the dark at room temperature before measuring emitted fluorescence (650-685 nm) with FMAT 2.0.1 software.

Western Blotting

23. Total cell pellets were lysed in buffer (50 mM Tris-Cl, pH 8.0/150 mM NaCl/1% Nonidet P 40/1 mM phenylmethylsulfonyl fluoride/0.045 mg/ml aprotinin). Aliquots of sample lysates or purified GPNMB protein were subjected to electrophoresis on Bis-Tris SDS polyacrylamide gel and blotted onto polyvinylidene difluoride (PVDF) membranes according to the standard method (28). Nonspecific binding sites were blocked by using 3% nonfat milk in PBS-0.05% Tween 20. Incubations with primary antibodies were carried out overnight at 4°C

with rabbit anti-GPNMB antiserum #2640 (5 μg/ml) or MAbs (10 μg/ml) in PBS-0.05% Tween 20 containing 1% milk; irrelevant IgG_1 or IgG_{2b} was used to control for non-specific binding. After washing membranes, specific protein bands were detected using HRP–linked secondary antibodies (Amersham Biosciences, UK) and developed with SuperSignal West Pico Chemiluminescence Kit (Pierce, Rockford, IL) according to manufacturer's instructions.

Indirect Analytical Flow Cytometry (IAFC)

24. Our standard procedures for these assays have been published extensively (22, 27, 29, 30). IAFC was performed as previously described (30) on a Becton Dickinson FACSort equipped with Lysys software (Becton Dickinson, San Jose, CA). Assays were performed at 4°C; all washes were performed with iced medium to facilitate the detection of cell surface receptors without allowing internalization to occur. As profiles obtained with cells maintained in ice cold 1% BSA-PBS or 0.5% paraformaldehyde-PBS were identical, the latter suspension buffer post secondary reagent was selected for longer-term stability. The percentage of a population designated as positive was arbitrarily defined as that region in which only the highest fluorescing 10% of the isotype control-stained cells graphed, corrected for background; this is a conservative estimate of the total positive staining population.

25. To examine the cell surface expression of GPNMB proteins, target cultured or biopsy-derived GBM cells were stained with anti-GPNMB MAbs, G11 or U2, or rabbit polyclonal Ab #2640 under non-permeabilized conditions as described previously (30). Subconfluent cells were detached from culture flasks by incubation with 0.02% EDTA/PBS; 1 × 106 cells were maintained in 0.5% paraformaldehyde/PBS for 10 minutes at 4°C, washed, resuspended in 150 μl of PBS containing 10% FBS, and blocked for 20 minutes at 4°C. After

two washes, the samples were reacted with anti-GPNMB MAbs (10 μg/ml) or rabbit polyclonal Ab #2640 (5 μg/ml) and irrelevant mouse IgGs (10 μg/ml) or rabbit IgGs (5 μg/ml) in PBS. After two additional washes, cells were incubated with FITC-labeled secondary antibody for 30 minutes at 4°C and analyzed on a Becton Dickinson FACSort instrument (Becton Dickinson, San Jose, CA).

Quantitative FACs Determination of Receptor Density

26. The number of GPNMB molecules expressed per cell by cell populations was determined by quantitative FACs determination of receptor density (QFACs) using the Quantum Simply Cellular™ system (Bangs Laboratories, Fishers, IN) as described (30). The microbead solution used is a mixture of five uniform populations which have varying capacities to bind no or serially increasing amounts of murine IgG; incubation of the bead sample with an identical aliquot of fluoresceinated MAb used for cell analysis allows extrapolation of antibody molecules bound/cell, and assuming 1:1 stoichiometry, of the number of receptors present, expressed as a population mean or median. Analysis of receptor density was performed by interpolation with the bead standard curves using QuickCal™ software (Bangs Laboratories); positive population percent was determined as described above for indirect analysis. The techniques for disaggregation of biopsy and xenograft-derived cells and preparation for flow cytometry have been thoroughly described (30).

Affinity Constant Determination by Surface Plasmon Resonance

27. Purified $GPNMB_{ECD}$ protein was immobilized on the surface of biosensor chips for analysis by using the BIAcore™3000 (BIAcore, Inc., Piscataway, NJ). Coupling of antigen was achieved using N ethyl-N'-(3-dimethylaminopropyl) carbodiimide/N-hydroxysuccinimide

according to the manufacturer's instructions. The running buffer was 10 mM HEPES/150 mM NaCl/3.4 mM EDTA, pH 7.4. The MAb samples were passed over the biosensor chip at concentrations from 200 to 1000 nM. The association and dissociation rate constants (k_{assoc} and k_{diss}) and average affinity were determined by using the nonlinear curve-fitting BIAevaluation software. KA at equilibrium was calculated as $K_A = k_{assoc} / k_{diss}$.

Iodination, Immunoreactive Fraction Determination, and Scatchard Analysis

28. Details of these procedures have been previously published (27, 31, 32). Purified MAbs were iodinated by the Iodogen method (31) to a specific activity of 1 to 3 μCi/μg Ig. The immunoreactive fraction (IRF) was conventionally determined by Lindmo analysis (33) using increasing amounts of positive (THRG) or negative (P3X63/Ag8.653) cells as targets in an 18- to 24-hour assay at 4°C. In a single assay of MAb G11, IRF was determined vs. GPNMB protein coupled to magnetic beads (34). Plotting the total divided by the specifically bound activity vs. the reciprocal of the antigen concentration yielded a linear plot, the intercept of which represents the inverse of the IRF. A modified Scatchard analysis was used to measure the binding affinity of iodinated MAbs beginning with serially diluted, labeled MAb starting at 10 μg/ml versus THRG MG cells, incubation at 4°C for 4 hours, and measurement of cell-bound activity as a proportion of input activity; nonlinear regression analysis to calculate K_A was performed with GraphPad Prism software (GraphPad Prism Software; San Diego, CA).

Tumor Samples

29. Samples of primary brain tumors were obtained from 90 newly diagnosed GBM patients from the Preston Robert Tisch Brain Tumor Center Tissue Bank, Duke University Medical Center, Durham, NC. The tumors were histologically diagnosed and graded as GBM,

according to WHO criteria (35). Among those 90 GBM patient samples, 50 cases were studied in quantitative real-time PCR analysis for *gpnmb* mRNA transcript detection, 79 GBM cases were analyzed by immunohistochemistry staining using anti-GPNMB antibodies, and 39 cases were done by both analyses. No patient had any history of chemotherapy or radiotherapy before surgery. The samples were immediately snap-frozen in liquid nitrogen and stored at -80°C until analysis.

Immunohistochemistry

30. Immunohistochemical (IHC) analysis of acetone-fixed (–70°C, 30 seconds) 5- to 8-μm frozen tissue sections of human tumor tissue was performed as described previously (22, 30). For detection of GPNMB, exposure to primary reagent (polyvalent rabbit antiserum #2640/irrelevant negative control rabbit IgG, or MAb G11/murine IgG2b isotype control at 10 and 5 μg/ml) was performed for 1 hour at room temperature. Slides were washed in PBS, the appropriate dilution of biotinylated goat anti-mouse IgG or goat anti-rabbit IgG (Vector) established by previous titration was applied, and the slides were incubated for 1 hour. Slides were washed again in PBS, exposed to HRP-avidin complex (Vector, Standard ABC Kit) for 30 minutes, and following PBS washes, developed with diaminobenzidine (Metal Enhanced DAB Substrate Kit, Pierce, Rockford, IL). Slides were counterstained with hematoxylin, dehydrated, mounted, and read independently by two investigators, including a neuropathologist. Slides were scored on the basis of staining intensity (none to intense, 0–3), and staining distribution and localization (0%–25%, 1+; 26%–50%, 2+; 51%–75%, 3+; 76%–100%, 4+), with notation of parenchymal, perivascular, or nuclear staining. Positive tissue control was provided by D256 MG athymic rat xenografts.

Statistical Analysis

31. The relationship between relative *gpnmb* mRNA expression levels ($gpnmb_{wt}$, $gpnmb_{sv}$, and $gpnmb_{wt+sv}$) and IHC score was examined using Spearman's correlation coefficient (scc). For survival analyses in which patient survival was computed from the date of pathology sample to date of death or last contact, relative *gpnmb* mRNA expression levels and IHC scores were categorized as ≤ 3.0 fold vs. > 3.0 fold and zero vs. positive, respectively. Survival data were current as of August 19, 2005. Cox e proportional hazards model analysis was used to check the statistical significance for each individual predictor of survival (SAS Statistical Analysis Package, Cary, NC). A predictor was considered for the multivariate model if the p-value was less than or equal to 0.25 in the univariate model. Age was included as a continuous predictor in the model due to a lack of dichotomy.

Alternative Splicing of GPNMB RNA Transcripts in Glioma Cells

32. We cloned the *gpnmb* gene from the human glioblastoma cell line D392 MG by isolation of poly-A mRNA and RT-PCR (Exhibit 1). Through the cDNA sequence analysis of individual clones, in addition to the published *gpnmb* RNA sequence (14), we found that one clone, EX1, had an in-frame insertion of a 36-bp fragment at nucleotide position 1019 in the ECD of *gpnmb* (Exhibit 1). By BLAST search (NCBI, Bethesda, MD), we determined that this 36-bp fragment insert created by alternative splicing completely matches the human genomic *gpnmb* intron DNA clone CTA-271G31 from chromosome 7 (GenBank No. NT033965). This 12 amino acid insertion variant is designated as $gpnmb_{sv}$ (splice variant), and the normal gene as $gpnmb_{wt}$ (wild type). In CTA-271G31, an additional 99 bp matching the GPNMBwt cDNA sequence was found directly downstream from this 36 bp-fragment. Further sequence analysis

revealed that CTA-271G31 contains the human genomic GPNMB sequence. The 5′ and 3′ ends of each intronic fragment matched the consensus sequences for 3′ acceptor site and for 5′ donor site (36, 37), confirming that GPNMBsv is generated by the alternative splicing of *gpnmb* RNA transcripts.

Quantification of *gpnmb* mRNA in GBM Cell Lines, Xenografts, and Biopsy Samples

33. After our initial screening analyses (13), we used real-time RT PCR to measure the expression of the *gpnmb* gene in seven GBM cell lines, four melanoma cell lines, seven malignant glioma xenografts, and 39 cases of newly diagnosed GBM samples (Exhibit 2 and Table 1; Exhibit 7) . First, human GBM-derived cell lines and melanoma cell lines were analyzed for *gpnmb* mRNA expression (Exhibit 2B). We designed specific primer sets to identify the expression of $gpnmb_{wt}$, $gpnmb_{sv}$ as well as $gpnmb_{wt+sv}$ (Exhibit 2A and details in the paragraphs above). As shown in Exhibit 2A, all seven glioma cell lines examined expressed both types of *gpnmb* RNA transcripts, that is, the wild-type $gpnmb_{wt}$ and the splice variant $gpnmb_{sv}$. By quantitative real-time RT-PCR, D54 MG, D392 MG, and D247 MG cells exhibited high levels of overall *gpnmb* mRNA, while U251 MG, T98G, and D245 MG exhibited moderate to marginal levels, and U87 MG exhibited very low or no *gpnmb* mRNA expression. See Exhibit 2B. Therefore, we used D54 MG, D392 MG, and D247 MG cells in studies of GPNMB protein expression.

34. For the melanoma cell lines we obtained from ATCC, C32, Malme-3M and SK-mel-28 exhibited high levels of *gpnmb* RNA expression ranging 20 to 60 fold higher relative to normal brain tissue by using β-actin as an internal control (Exhibit 2B); however, A375 melanoma line expressed low level of *gpnmb* RNA. We also found that malignant glioma

xenografts D256 MGX and 12A-7 exhibited a 3-fold increase over normal brain samples (Exhibit 2B).

35. Real time RT-PCR analysis of $gpnmb_{sv}$ alone in the same cell line panel revealed that a subset of $gpnmb_{wt}$ positive cell lines also express $gpnmb_{sv}$. Relative transcript levels of $gpnmb_{sv}$ RNA were 10- to 100-fold lower than those for $gpnmb_{wt}$, and no significant $gpnmb_{sv}$ or $gpnmb_{wt}$ transcripts were detected in normal brain samples. Similar analysis of established glioma cell lines revealed that significant levels were present in three potential glioma target cell lines, D247 MG, D392 MG, and D54 MG; the latter two were chosen as reference controls on the basis of reproducible growth *in vitro*.

36. Going from cultured cell lines to patient tumors, we measured *gpnmb* mRNA levels in 50 GBM biopsy samples. We found that 35/25 (70%) cases were positive (at least 3-fold increase over normal whole brain sample) for $gpnmb_{wt + sv}$ mRNA, 26/50 (52%) cases were positive for $gpnmb_{wt}$ mRNA, and 15/50 (30%) cases were positive for $gpnmb_{sv}$ mRNA (Table 1; Exhibit 7).

37. High transcript expression (a greater than 10-fold increase over normal brain of $gpnmb_{wt + sv}$ mRNA transcripts) was found in 19/50 (38%) cases; for $gpnmb_{wt}$ and $gpnmb_{sv}$ mRNA, high expression was found in 11/50 (22%) and 3/50 (6%) biopsy samples, respectively, as shown in Table 1 (Exhibit 7). As the $gpnmb_{wt}$ mRNA profile was virtually identical to the $gpnmb_{wt + sv}$ profile, it is conceivable that $gpnmb_{wt}$ is the predominant detected moiety. No significant expression for the *gpnmb* gene was detected in normal brain samples assayed simultaneously.

Isolation and Quantitative Analyses of anti-GPNMB Antibodies for Cell Surface GPNMB

38. Though high levels of RNA transcripts can be predictive of protein levels, the presence of detectable protein in human tumor material must be established for targeting applications. Thus, we developed specific antibodies to detect the presence of GPNMB protein. Purified rabbit anti-GPNMB IgG #2640 was demonstrated to detect the cell surface GPNMB protein by performing the indirect FACs analysis as shown in Exhibit 3A.

39. Anti-serum #2640 reacted with GPNMB positive cell lines D392 MG and D54MG, as indicated by *gpnmb* RNA expression, but not with a negative cell line such as HEK293 (Exhibit 3A) or U251 MG cell lines. Anti-serum #2640 also reacted with a GPNMB transfected HEK293 cell line, which expressed GPNMB on the cell surface (Exhibit 3A, right panel).

40. In addition, we immunized three different standard mouse strains (Balb/c, C57Bl/6, and C3H/He) by the intradermal route with cytomegalovirus-based plasmid DNA (pDNA) encoding the ECD of normal $gpnmb_{wt}$ or $gpnmb_{sv}$. Those animals were subsequently boosted intraperitoneally with bacterially expressed or insect cell–expressed $GPNMB_{ECD}$ protein. Two separate fusions were performed as described in the paragraphs above. As derivation of MAbs specific for the extracellularly expressed portion of GPNMB was desired, supernatants from outgrowing hybridomas were screened for reactivity on the D54MG cell line and GPNMB-transfected cell line THRG, previously shown to express GPNMB (20, 21); U251 MG, which does not express GPNMB, was used as the negative control in FMAT screening. From the two protocols, two hybridomas (B: IgG_{2b} MAb G11; U: IgG_{2b} MAb U2) were selected for cloning and further analysis.

41. Detection of cell surface GPNMB was performed with anti-GPNMB MAb G11. Representative indirect FACs histograms of purified MAb G11 are shown in Exhibit 3B; this analysis establishes that MAb G11, generated following immunization with pDNA of GPNMB and with bacterially produced GPNMB protein, is reactive with a cell surface epitope on the purposefully transfected THRG cell line and on D54 MG. See Exhibit 3B.

42. Indirect FACs analysis revealed reactivity of G11 with GPNMB-expressing D247MG cells under non-permeabilized conditions (Exhibit 3B, middle panel). Furthermore, stable transfectant D247 MG-GPNMB showed a peak shift compared to that of the parental line D247 MG, indicating an increase in the number of surface GPNMB molecules after transfection. Irrelevant control IgG_{2b} was unreactive with both lines. Similar profiles were obtained with all of the components of this MAb panel on SK-Mel-28 cell lines; the non-cell surface GPNMB-expressing cell line U251 MG was negative with these MAbs detected by FACS.

43. MAbs G11 and U2 were fluoresceinated for QFACs analysis, and cell surface GPNMB densities were determined on a panel of cell lines, disaggregated xenografts, and biopsy samples. MAb U2 was determined to be the optimal FITC-labeled reagent for these analyses. An example of such an analysis of patient biopsy GBM 2180 is provided in Exhibit 3B (right panel); from the regression equation calculated for FITC-MAb binding to quantitated receptor site beads, the fluorescent channel value obtained with GBM 2180 cells predicts a median GPNMB density of 7×10^4 GPNMB molecules/cell. Fifty percent (4/8) of long-term cultured GBM cell lines expressed GPNMB in excess of 1×10^4 molecules/cell; only 3/9 established xenografts did so. Analysis of freshly disaggregated cells from GBM (n = 27) biopsies revealed that 11/27 (41%) of GBM expressed cell surface GPNMB with a range of densities from 1.1 to

7.8×10^4; one GBM expressed > 105 GPNMB molecules per cell. Positive GPNMB-expressing cell lines THRG and SK-Mel-28 exhibited 1.4 to 3.9 × 105 and 3 to 9×10^4 GPNMB molecules per cell, respectively. No GPNMB expression was detected by QFACs in medulloblastoma cultured cells, xenografts, or biopsies.

Detection of GPNMB Protein by Western Blotting in Glioblastoma Cells

44. The integrity of the GPNMB coding sequence was first investigated by expressing the recombinant protein in insect cells. By Western blotting, purified rabbit anti-GPNMB IgG #2640 reacted with the lysates of Sf9 insect cells transiently transfected with the ECD of GPNMB (Exhibit 3C, left panel). $GPNMB_{ECD}$ expressed in Sf9 cells migrated with an apparent molecular weight of Mr ~ 70 kDa, which was significantly larger than the molecular weight of $GPNMB_{ECD}$ protein deduced from the amino acid composition (54 kDa). The ECD of human GPNMB contains 12 potential N-glycosylation sites; N-glycosidase treatment of Sf9 lysates significantly reduced the molecular size of $GPNMB_{ECD}$ almost identical to that produced in *Escherichia coli* (Exhibit 3C, left panel), indicating that the discrepancy in the molecular mass is due to glycosylation of the GPNMB protein.

45. We further investigated the GPNMB protein expression in cultured human GBM cell lines. Detection of GPNMB proteins using antiserum #2640 was carried out in several cultured human GBM cells, including D392 MG and D54 MG as shown in Exhibit 3C (middle panel). In GBM cell lines, GPNMB proteins were detected by antiserum #2640 in D392 MG and D54 MG as multiple bands between ~80 kDa and ~100 kDa as shown by arrow lines and a faint band at 120 kDa. This is shown in the middle panel of Exhibit 4A. We also found two non-specific bands reacted with #2640 as shown by arrow heads at 70 kDa and 40 kDa positions.

46. The GPNMB protein expression increased significantly after transfection of U251MG, D54MG, or D247MG cells with GPNMB expression vectors. The proteins appeared as multiple bands in Western blots, presumably due to different degrees of glycosylation; essentially, the GPNMB proteins migrated predominantly as two bands of apparent molecular weights Mr ~100 kDa and ~ 75kDa. In addition, Western blot of a parent control line HEK293 and its GPNMB transfectant with #2640 indicated that two non-specific bands were also seen in the negative control; however, the Western blot results of HEK293/GPNMB transfectant lysate exhibited highly specific reactivity to recombinant GPNMB protein as shown in Exhibit 3C (right panel).

47. To establish the restricted specificity of these MAbs, Western blots were performed using the glycosylated purified $GPNMB_{ECD}$ isolated from Sf9 cells as control and cell lysates prepared from the U251MG cell line as well as the GPNMB-transfected cell lines, U251MG and D247MG. As shown in Exhibit 3D, MAb G11 recognized the purified $GPNMB_{ECD}$ protein (~ 70 kDa mass, small arrow). MAb U2 exhibited similar pattern. All MAbs detected bands between approximately 75-100 kDa and 120 kDa in the GPNMB-transfected D247MG line in a pattern similar to that of rabbit polyclonal antiserum #2640 (Exhibit 3C and 3D). MAb G11 was capable of consistently identifying these bands in the untransfected glioma cell lines, U251MG and D54MG, as well as their GPNMB-transfectants in a pattern similar to that of rabbit polyclonal antiserum #2640 while IgG_{2b} irrelevant isotype control was negative (Exhibit 3D).

Kinetics of MAb-to-GPNMB Binding

48. A kinetic analysis of the interaction of purified MAbs with immobilized $GPNMB_{ECD}$ by surface plasmon resonance (BIAcore) was conducted to determine the association and dissociation rate constants and calculation of the affinity constants. Determination of the association and dissociation rates from the sensorgrams reveals a k_{assoc} of 1.1 × 106 (1/Ms) and a k_{diss} of 1.1×10^{-3} (1/s) for MAb G11. The K_A at binding equilibrium, calculated as $K_A = k_{assoc}/k_{diss}$, is 9.6×10^8 (1/M) for G11 and 2.7×10^7 (1/M) for U2. Anti-GPNMB MAbs G11 and U2 were also each analyzed by conventional Scatchard analysis vs. the THRG cell line. MAbs G11 and U2 exhibited KA values of 1.7×10^8 M-1 and 2.1×10^8 M-1, respectively, measured by Scatchard analysis vs. cell surface expressed GPNMB and IRFs in the range of 75% to 91% for G11 and 71% to 75% for U2, respectively. The estimated cell surface receptor densities obtained from the βmax values for G11 and U2 were quite similar (ranges of $4–8 \times 10^4$) in multiple assays.

Immunohistochemical Analysis

49. The immunohistochemical (IHC) analysis of GBM tissue samples from newly diagnosed, pre-therapy patient cases was performed using rabbit anti-GPNMB serum #2640 and/or MAb G11 to stain frozen sections of the tumor samples (39 GBM) that were also used for GPNMB mRNA analysis. The Spearman's analysis (one sided, assuming a direct relationship between mRNA presence and production of protein) revealed that the correlation of GPNMB mRNA and protein expression was significant ($p < 0.0001$); the higher the detected level of mRNA, the more probable a positive immunohistochemistry result; Spearman's correlation coefficients equal to 0.58 and 0.57 for all ages and those greater than 45, respectively.

50. In addition to those 39 GBM cases, an additional 40 GBM were stained with rabbit anti-GPNMB serum #2460; of these total 79 cases, 32 GBM were concurrently stained with MAb G11 and appropriate irrelevant IgG_{2b} isotype control. Results of this analysis are summarized in Table 2 (Exhibit 8) (79 cases of GBM) and are illustrated in Exhibit 4 for some representative cases. A high percentage of positive anti-GPNMB staining was observed in those 79 patient samples; 52 out of 79 (66%) were stained as positive (Table 2; Exhibit 8). As shown in Exhibit 4, GPNMB localization can present in different patterns; while the majority of cases (58%, Table 2; Exhibit 8) exhibit focal or multifocal tumor parenchymal staining panels (E, H, I, and K) with clear membrane staining (panels E, F, and K), a subset of GBMs (42%, Table 2; Exhibit 8) exhibits pronounced perivascular accumulation of GPNMB either with (27%, panels B and C) or without (15%) accompanying parenchymal staining.

Survival Analysis

51. Analyses were conducted to examine the effect on survival of select predictors (RNA expression and IHC data) in specific patient subgroups: 39 newly diagnosed GBM patients (Tables 3A-3C; Exhibit 9) and a subgroup of patients older than 45 years (data not shown, n=34). Among all 39 patients, the relative $gpnmb_{wt+sv}$ RNA expression level was a strong predictor of survival across all analyses as shown in Exhibit 5A. The hazard of death for patients with relative $gpnmb_{wt+sv}$ RNA expression level greater than 3.0 fold was 2.98 (95% CI: 1.26 – 7.06) as shown in Table 3A (Exhibit 9). The estimated 2 year survival probability was 0.42 (95% CI: 0.21 – 0.81) for patients with relative $gpnmb_{wt+sv}$ RNA expression levels less than or equal to 3 fold, and 0.15 (95% CI: 0.06 – 0.37) for patients with relative $gpnmb_{wt+sv}$ RNA expression level greater than 3.0 fold. The median patient survival for low $gpnmb_{wt+sv}$ RNA

expression level (< 3 fold of normal brain sample) and high $gpnmb_{wt+sv}$ RNA expression level (> 3 fold) are 90 and 55 weeks, respectively (Table 3B; Exhibit 9). For patients older than age 45, the 2-year survival estimate was 0.40 and 0.13 for the low $gpnmb_{wt+sv}$ RNA and high $gpnmb_{wt+sv}$ RNA groups, respectively (Cox hazard ratio of 3.00 [95% CI: 1.19–7.57]). The median patient survival for low $gpnmb_{wt+sv}$ RNA expression level (< 3 fold of normal brain sample) and high $gpnmb_{wt+sv}$ RNA expression level (> 3 fold) are 94 and 55 weeks, respectively .

52. The relative $gpnmb_{wt}$ RNA expression level was also a strong predictor of survival. The hazard of death for patients with relative $gpnmb_{wt}$ RNA expression level greater than 3.0 fold was 2.21 (95% CI: 1.08 – 4.55) as shown in Table 3A (Exhibit 9). The estimated 2-year survival probability was 0.35 (95% CI: 0.19 – 0.64) for patients with relative $gpnmb_{wt}$ RNA expression levels less than or equal to 3.0 fold, and 0.11 (95% CI: 0.03 – 0.39) for patients with relative $gpnmb_{wt}$ RNA expression levels greater than 3.0 fold (Table 3B; Exhibit 9). For patients older than 45 years, the survival probability at 104 weeks for low levels of $gpnmb_{wt}$ RNA was 0.35, whereas the probability for high levels of $gpnmb_{wt}$ RNA, 0.06 (Cox hazard ratio of 2.38 [95% CI: 1.09–5.20]).

53. In addition, immunohistochemistry score was also a strong predictor of survival as shown in Exhibit 5B. The hazard of death for patients with a positive IHC score was 2.80 (95% CI: 1.24 – 6.32); i.e., patients with positive IHC staining have higher risk of death (2.80 times) than patients with negative staining (Table 3A; Exhibit 9). The estimated 2-year survival probability was 0.39 (95% CI: 0.19 – 0.77) for patients with zero IHC scores and 0.15 (95% CI: 0.06 – 0.38) for patients with positive IHC scores. The median patient survival for negative GPNMB IHC staining and positive GPNMB IHC staining are 90 and 50 weeks, respectively

(Table 3B; Exhibit 9). For patients older than 45, the 2-year survival estimate was 0.36 and 0.13 for the zero and positive IHC groups, respectively (Cox hazard ratio of 2.71 [95% CI: 1.14–6.45], data not shown).

54. Due to multicollinearity in a Cox model with age, immunohistochemistry and mRNA expression levels as predictors, two bivariate models containing age have been generated (Table 3C; Exhibit 9). The first model demonstrates that patients with high relative GPNMBwt RNA expression levels have a higher risk of death (2.6 times higher) than patients with low relative GPNMBwt RNA expression level after adjusting for age. The second model demonstrates similar results with positive immunohistochemistry scores that patients with positive GPNMB IHC score have a higher risk of death (2.6 times higher) than patients with zero IHC score after adjusting for age.

55. Effective MAb-based targeted therapy depends on several factors, which include characteristics of the target antigens, the immune reagents used, the route of administration and the tissue dynamics of the tumor (8). Preferential expression on or around tumor cells and membrane localization are major requirements for tumor antigens in antibody therapy (3, 8). This declaration presents data indicating that the transmembrane glycoprotein GPNMB is overexpressed in a significant portion of high-grade glioma tumors, at both the mRNA and the protein levels, but not in normal brain tissues. We performed genetic and immunohistochemical evaluation of human gliomas to determine incidence, distribution, and pattern of localization of GPNMB antigens in brain tumors. We used quantitative RT-PCR to analyze 50 newly diagnosed human GBM biopsy samples received directly from surgery to determine levels of mRNA for $gpnmb_{wt}$ + $gpnmb_{sv}$. The results revealed that 70% of GBM patient samples were

positive for *gpnmb* transcripts and that 38% of GBM showed a greater than 10-fold increase over normal brain in *gpnmb* mRNA expression. In contrast, only marginal levels of *gpnmb* mRNA were noted in normal brain RNA.

56. Correlation between the assays was good, as Spearman's analysis (one sided, assuming a direct relationship between mRNA presence and production of protein) revealed that the correlation of *gpnmb* mRNA and protein expression as detected by immunohistochemistry was significant; that is, the higher the detected level of mRNA, the more probable a positive immunohistochemistry result. However, the sensitivity of mRNA detection is far higher than that of immunohistochemical assays, which accounts for some of the discrepancies noted. In cases where protein is detected in tissue in the absence of mRNA, the most likely explanation is that the mRNA is short-lived and chronically produced, leaving a relatively long-lived protein *in situ* (38). GPNMB antigens exhibit diffuse staining in frozen sections with distinct membrane staining and absence of blood vessel staining by both polyvalent rabbit antiserum and MAbs demonstrably specific for GPNMB. These observed staining patterns corroborate the cell membrane staining observed in QFACs assays as described above. These data demonstrate the establishment of specific and reliable antibody probes for analysis of tissue and biopsy-derived cell populations. Concerning subcellular localization, indirect FACS analysis with anti-GPNMB MAb G11 under nonpermeabilizing conditions demonstrated that GPNMB proteins are expressed at the surface cell membrane of human glioblastoma cell line D247 MG. Furthermore, a shift of peak was observed following stable transfection with full-length GPNMB, indicating an increase in the number of surface GPNMB protein molecules following transfection. This

supertransfectant cell line will likely prove useful in our preclinical MAb localization and tumor immunotherapy models.

57. Although some extracellular matrix antigens, such as tenascin, and some non-internalizing surface antigens are suitable for immunotherapeutic approaches, the ideal antigens for brain tumor immunotherapy would be those that fulfill the following criteria: (A) the general consensus for minimum surface antigen density is $\geq 1 \times 10^4$ protein molecules per cell (30, 39), (B) stability at the cell surface and lack of antigen shedding (8), and (C) internalization following binding to ligand or antibody (8). Glioma cell surface-expressed GPNMB fulfills these criteria in terms of adequate cell surface diversity, dynamics of protein synthesis, half-life, internalization, and mechanisms of degradation (8). Little is known about the distribution and function of GPNMB proteins in normal human organs (13, 14, 40). However, for tumors localized within the CNS, the optimal route for the administration of MAb-based therapeutic agents is through surgically created resection cavities or saturation of an entire hemisphere by intracranial microdiffusion (41). The expression of GPNMB in distant normal tissues should not compromise the compartmental delivery of GPNMB-related immunological agents within the CNS, because only small amounts of conjugates reach systemic organs (42).

58. The mechanistic biological significance of the aberrant expression of *gpnmb* in high-grade gliomas remains to be determined. In another study, the expression levels of *gpnmb* RNA transcripts showed a positive correlation with increasing grade of tumors . The GBM group exhibited higher *gpnmb* mRNA levels than those in AA; in addition, the appearance of perivascular accumulation of GPNMB protein was noted in GBM, but was absent in AA . The ECD of GPNMB contains 12 potential N glycosylation sites, an RGD integrin-binding motif,

and a heparin-binding motif (14). Other functional motifs found are a polycystic kidney disease motif and a proline-rich region that presumably forms a hinge and can mediate protein-protein interaction. In a genetically defined human glioma model using minimally transformed human fetal astrocytes (20), transfection of GPNMB resulted in the drastic change of tumor phenotype, with invasion of brain tissues and formation of spontaneous metastasis (21). Thus, GPNMB may serve as an adhesion molecule mediating cell-cell and/or cell-matrix interaction (15) and may contribute to the acquisition of the invasive nature of malignant glioma cells.

59. For survival analysis, newly diagnosed GBM patients over the age of 45 had a higher risk of death, as has been known for decades. Similarly, in this population univariate analyses show that patients with high relative GPNMB mRNA expression levels (wt and wt+sv) had a higher risk of death. The relative GPNMB protein expression levels (positive and negative IHC results) held the same significance. Taken together, the results of survival analysis suggest that the relative GPNMB mRNA levels and IHC staining represent a strong prognostic predictor of poor GBM patient survival. There are only a few molecular markers that are prognostic for survival in malignant gliomas. High GPNMB expression in GBM patient samples, strong GST-π protein expression in human gliomas (43), and a functional polymorphism in EGF gene (44) are associated with clinically more aggressive gliomas and are useful and powerful prognostic markers of poor patient survival.

60. In conclusion, increased *gpnmb* mRNA levels correlated strongly with elevated GPNMB protein expression in GBM biopsy samples and higher risk of death. Statistically significant predictors of survival among patients with GBM are age, the mRNA expression variables (wt and wt+sv), and IHC positivity. In a Cox model examining RNA for the subgroup of patients over 45 year old in these populations mRNA expression and IHC were shown to add significant prognostic value beyond that provided by age alone. These data indicate that GPNMB is a potentially useful tumor-associated antigen in immunotherapeutic approaches for malignant gliomas. We propose that therapeutic strategies designed to target GPNMB may be successful in malignant glioma treatment.

61. The statements I made in this declaration of my own knowledge are true and correct. I believe that the statements I made in this declaration based on information or belief are true and correct. I have been warned that willful false statements and the like can be punished by fine, imprisonment, or both (18 U.S.C. § 1001).

Dated: 15 Feb 06

Gregory J. Riggins

Gregory J. Riggins, M.D., Ph.D.

Exhibit 1

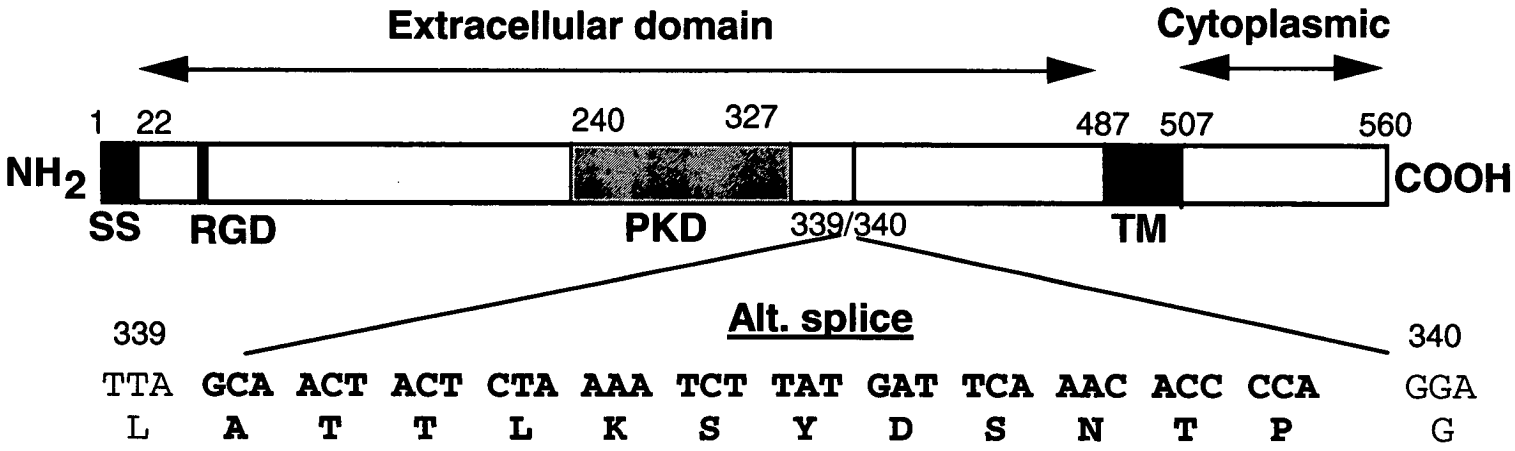

Schematic protein domain structure of human GPNMB and its alternatively spliced variant insertion in glioblastoma-derived cell lines. NH_2, amino terminus; SS, signal sequence; RGD, RGD tripeptide; PKD, polycystic kidney disease domain; TM, transmembrane segment; COOH, carboxyl terminus; amino acid residue numbers lie above and below the structure. **Alt. splice**, 12-amino acid insert generated by alternative splicing as described in this paper.

DNA sequence and predicated amino acid translation of the 36-bp insert segment are indicated.

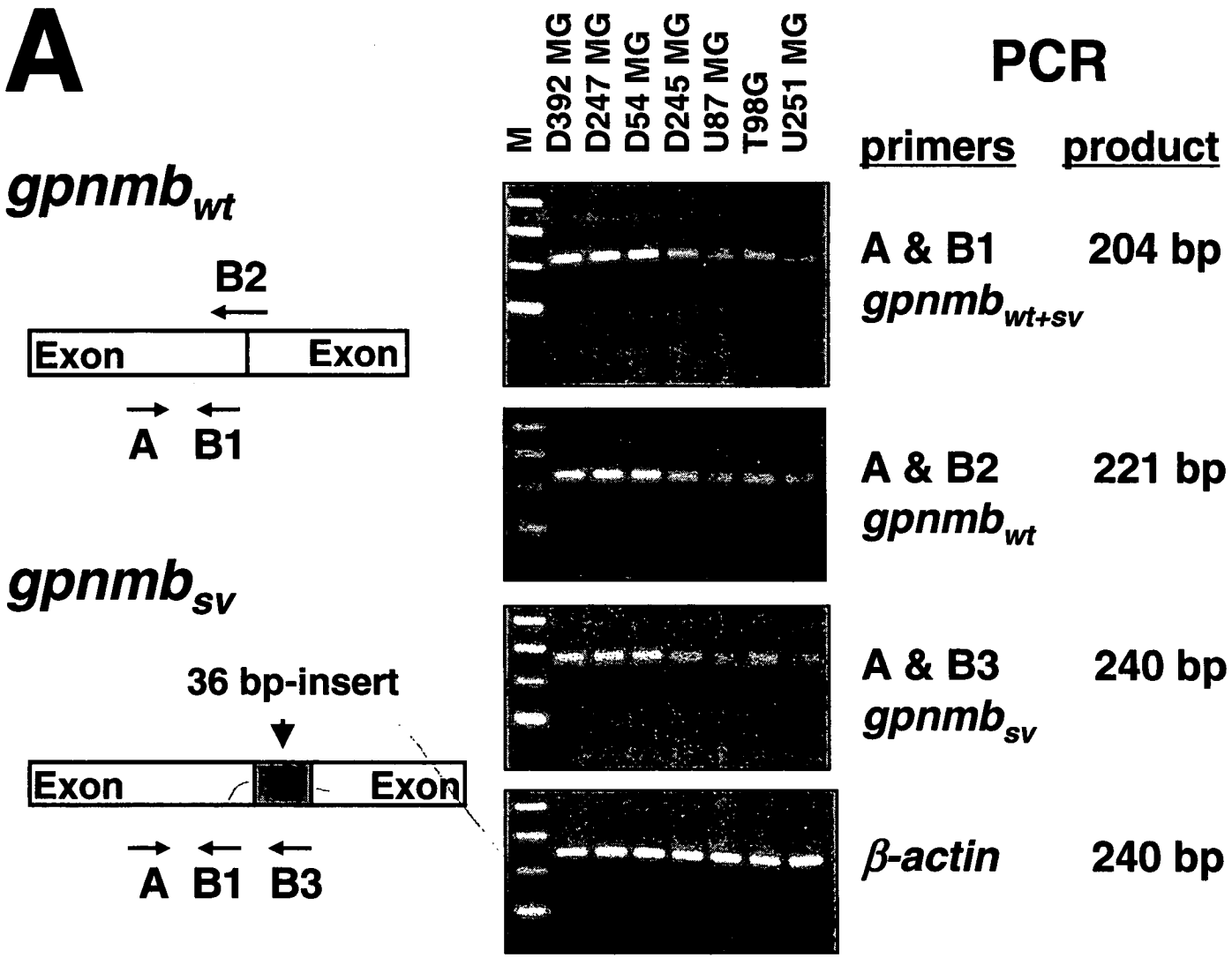
A
gpnmb wt
B2
Exon
Exon
A
B1
gpnmb sv
36 bp-insert
Exon
Exon
A
B1
B3
M
D392 MG
D247 MG
D54 MG
D245 MG
U87 MG
T98G
U251 MG
PCR
primers
product
A & B1
204 bp
gpnmb wt+sv
A & B2
221 bp
gpnmb wt
A & B3
240 bp
gpnmb sv
β-actin
240 bp

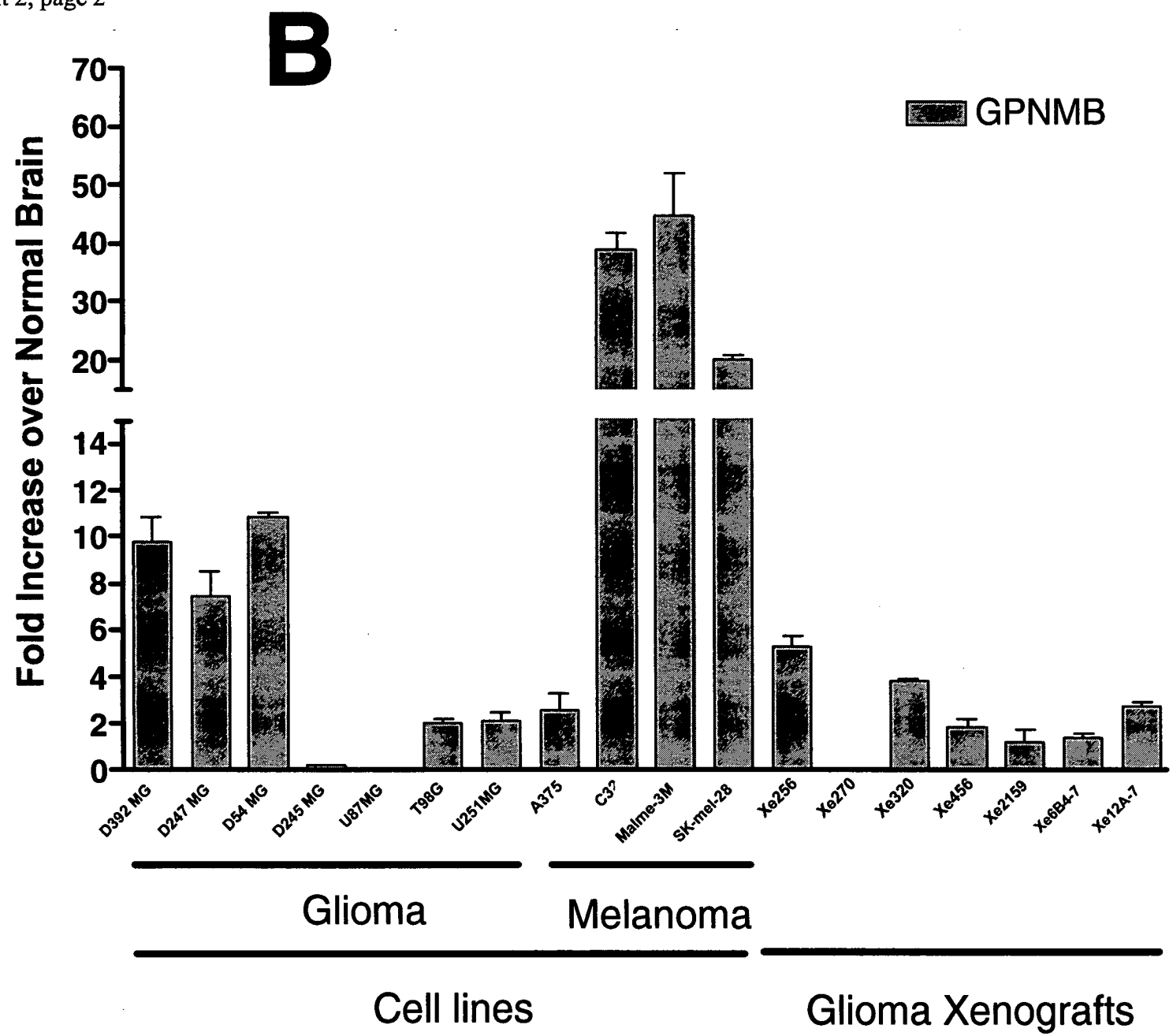
B
GPNMB
Fold Increase over Normal Brain
70
60
50
40
30
20
14
12
10
8
6
4
2
0
D392 MG
D247 MG
D54 MG
D245 MG
U87MG
T98G
U251MG
A375
C32
Malme-3M
SK-mel-28
Xe256
Xe270
Xe320
Xe456
Xe2159
Xe6B4-7
Xe12A-7
Glioma
Melanoma
Cell lines
Glioma Xenografts

A

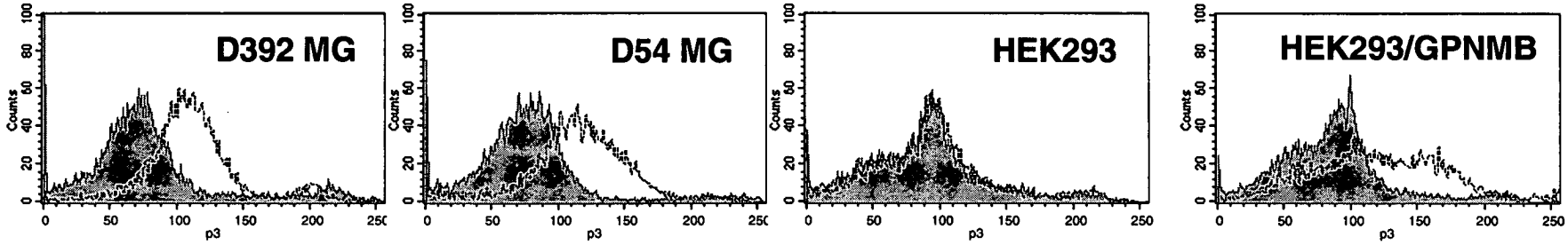
D392 MG
D54 MG
HEK293
HEK293/GPNMB
Counts
p3

B

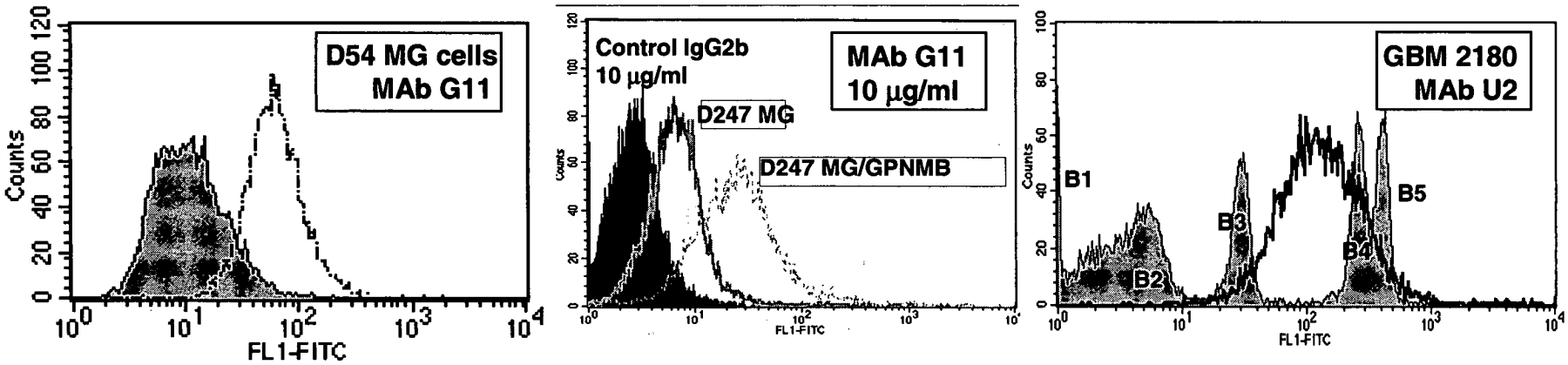
D54 MG cells
MAb G11
Counts
FL1-FITC
Control IgG2b
10 µg/ml
D247 MG
D247 MG/GPNMB
MAb G11
10 µg/ml
GBM 2180
MAb U2
B1
B2
B3
B4
B5

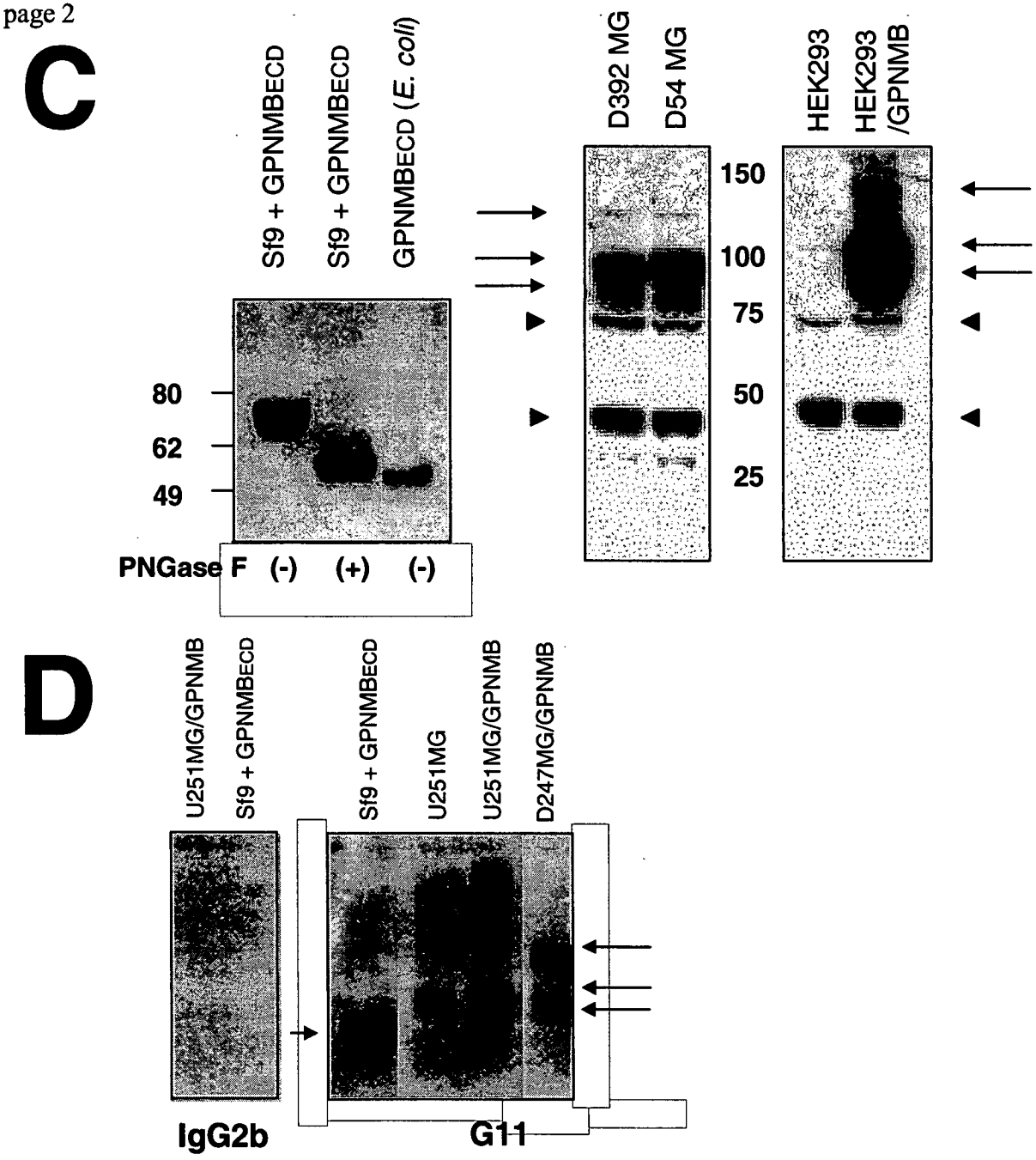
C
Sf9 + GPNMBECD
Sf9 + GPNMBECD
GPNMBECD (E. coli)
80
62
49
PNGase F (-) (+) (-)
D392 MG
D54 MG
HEK293
HEK293 /GPNMB
150
100
75
50
25
D
U251MG/GPNMB
Sf9 + GPNMBECD
Sf9 + GPNMBECD
U251MG
U251MG/GPNMB
D247MG/GPNMB
IgG2b
G11

Exhibit 4

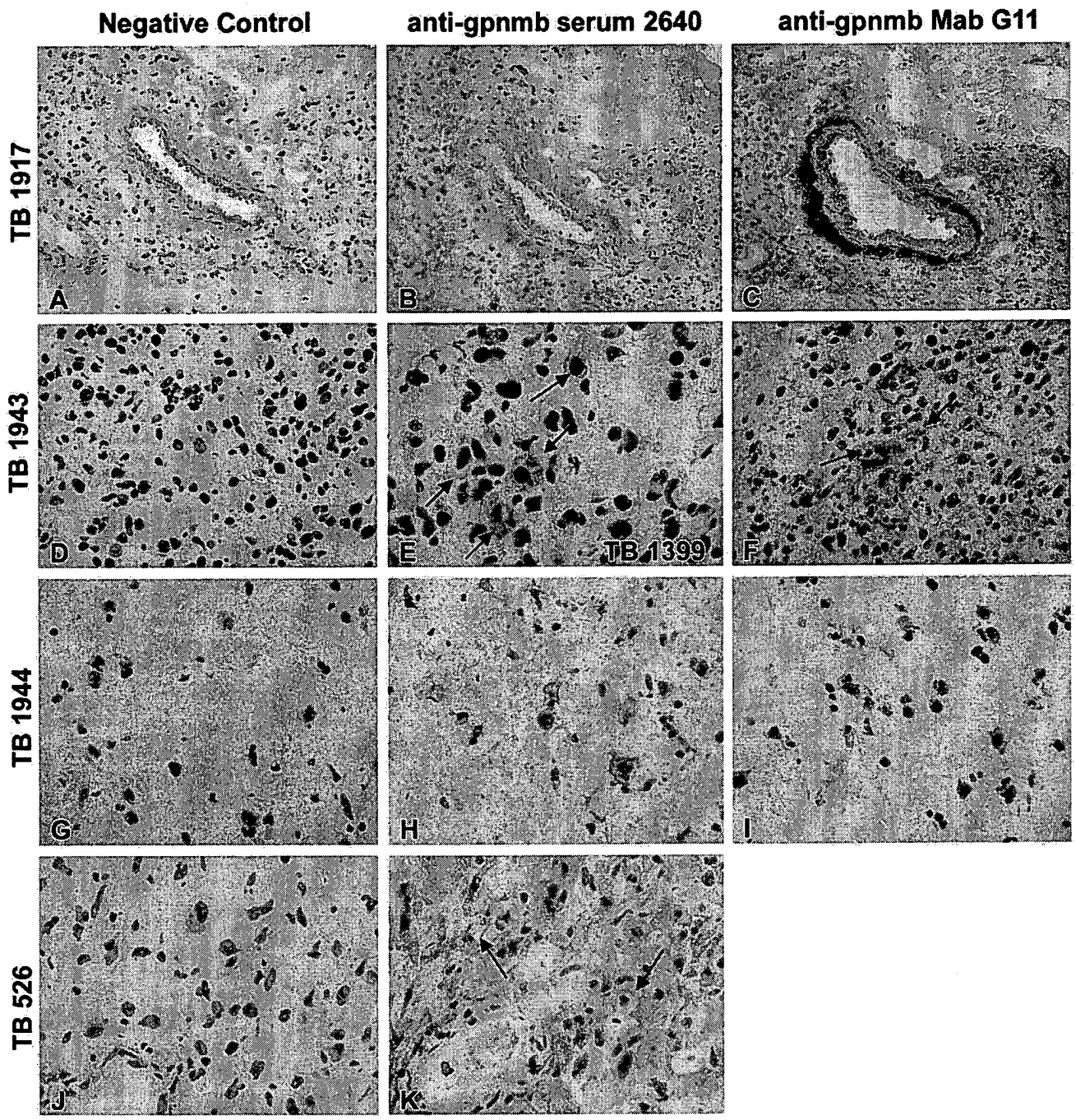
Negative Control
anti-gpnmb serum 2640
anti-gpnmb Mab G11
TB 1917
TB 1943
TB 1944
TB 526
A
B
C
D
E
TB 1399
F
G
H
I
J
K

Exhibit 5

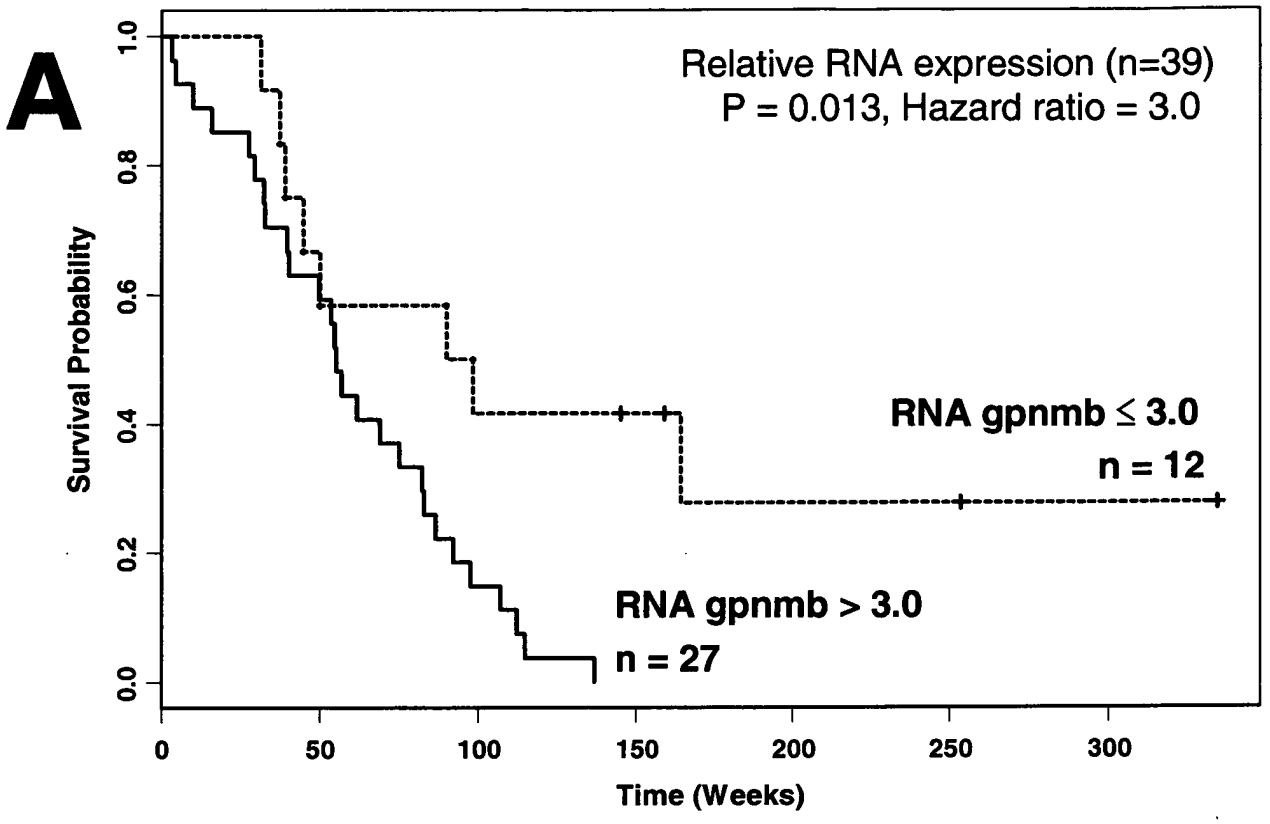
A
Relative RNA expression (n=39)
P = 0.013, Hazard ratio = 3.0
RNA gpnmb ≤ 3.0
n = 12
RNA gpnmb > 3.0
n = 27
Survival Probability
0.0
0.2
0.4
0.6
0.8
1.0
0
50
100
150
200
250
300
Time (Weeks)

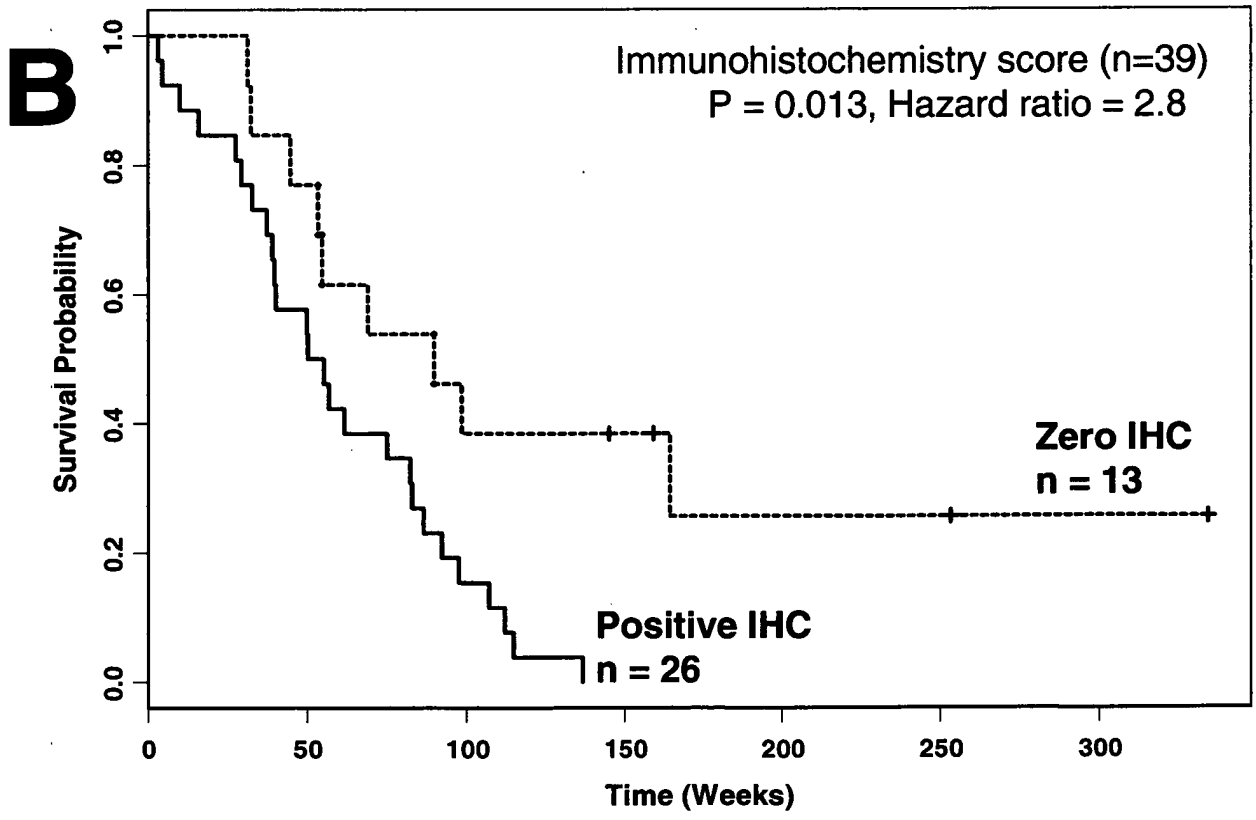
B
Immunohistochemistry score (n=39)
P = 0.013, Hazard ratio = 2.8
Zero IHC
n = 13
Positive IHC
n = 26
Survival Probability
0.0
0.2
0.4
0.6
0.8
1.0
0
50
100
150
200
250
300
Time (Weeks)

Exhibit 6. References

1. Berger MS, Leibel SA, Levin VA. Primary central nervous system tumors of the supratentorial compartement. In: Levin VA, editor. Cancer in the Nervous System. London: Churchill Livingston; 1996. p. 57-126.

2. Stupp R, Mason WP, van den Bent MJ, et al. Radiotherapy plus concomitant and adjuvant temozolomide for glioblastoma. N Engl J Med 2005;352:987-96.

3. Waldmann TA. Monoclonal antibodies in diagnosis and therapy. Science 1991;252:1657-62.

4. Kalofonos HP, Pawlikowska TR, Hemingway A, et al. Antibody guided diagnosis and therapy of brain gliomas using radiolabeled monoclonal antibodies against epidermal growth factor receptor and placental alkaline phosphatase. J Nucl Med 1989;30:1636-45.

5. Brady LW, Miyamoto C, Woo DV, et al. Malignant astrocytomas treated with iodine-125 labeled monoclonal antibody 425 against epidermal growth factor receptor: a phase II trial. Int J Radiat Oncol Biol Phys 1992;22:225-30.

6. Bigner DD, Brown MT, Friedman AH, et al. Iodine-131-labeled antitenascin monoclonal antibody 81C6 treatment of patients with recurrent malignant gliomas: phase I trial results. J Clin Oncol 1998;16:2202-12.

7. Kuan CT, Reist CJ, Foulon CF, et al. 125I-labeled anti-epidermal growth factor receptor-vIII single-chain Fv exhibits specific and high-level targeting of glioma xenografts. Clin Cancer Res 1999;5:1539-49.

8. Wikstrand CJ, Cokgor I, Sampson JH, Bigner DD. Monoclonal antibody therapy of human gliomas: current status and future approaches. Cancer Metastasis Rev 1999;18:451-64.

9. Bigner DD. Biology of gliomas: potential clinical implications of glioma cellular heterogeneity. Neurosurgery 1981;9:320-6.

10. Kleihues P, Ohgaki H. Primary and secondary glioblastomas: from concept to clinical diagnosis. Neuro-oncol 1999;1:44-51.

11. Wikstrand CJ, Bigner SH, Bigner DD. Demonstration of complex antigenic heterogeneity in a human glioma cell line and eight derived clones by specific monoclonal antibodies. Cancer Res 1983;43:3327-34.

12. Velculescu VE, Zhang L, Vogelstein B, Kinzler KW. Serial analysis of gene expression. Science 1995;270:484-7.

13. Loging WT, Lal A, Siu IM, et al. Identifying potential tumor markers and antigens by database mining and rapid expression screening. Genome Res 2000;10:1393-402.

14. Weterman MA, Ajubi N, van Dinter IM, et al. nmb, a novel gene, is expressed in low-metastatic human melanoma cell lines and xenografts. Int J Cancer 1995;60:73-81.

15. Shikano S, Bonkobara M, Zukas PK, Ariizumi K. Molecular cloning of a dendritic cell-associated transmembrane protein, DC-HIL, that promotes RGD-dependent adhesion of endothelial cells through recognition of heparan sulfate proteoglycans. J Biol Chem 2001;276:8125-34.

16. Safadi FF, Xu J, Smock SL, Rico MC, Owen TA, Popoff SN. Cloning and characterization of osteoactivin, a novel cDNA expressed in osteoblasts. J Cell Biochem 2001;84:12-26.

17. Kwon BS, Chintamaneni C, Kozak CA, et al. A melanocyte-specific gene, Pmel 17, maps near the silver coat color locus on mouse chromosome 10 and is in a syntenic region on human chromosome 12. Proc Natl Acad Sci U S A 1991;88:9228-32.

18. Turque N, Denhez F, Martin P, et al. Characterization of a new melanocyte-specific gene (QNR-71) expressed in v-myc-transformed quail neuroretina. Embo J 1996;15:3338-50.

19. Bachner D, Schroder D, Gross G. mRNA expression of the murine glycoprotein (transmembrane) nmb (Gpnmb) gene is linked to the developing retinal pigment epithelium and iris. Brain Res Gene Expr Patterns 2002;1:159-65.

20. Rich JN, Guo C, McLendon RE, Bigner DD, Wang XF, Counter CM. A genetically tractable model of human glioma formation. Cancer Res 2001;61:3556-60.

21. Rich JN, Shi Q, Hjelmeland MD, et al. Bone-related genes expressed in advanced malignancies induce invasion and metastasis in a genetically defined human cancer model. J Biol Chem 2003.

22. Wikstrand CJ, Stanley SD, Humphrey PA, et al. Investigation of a synthetic peptide as immunogen for a variant epidermal growth factor receptor associated with gliomas. J Neuroimmunol 1993;46:165-73.

23. Morgenstern JP, Land H. Advanced mammalian gene transfer: high titre retroviral vectors with multiple drug selection markers and a complementary helper-free packaging cell line. Nucleic Acids Res 1990;18:3587-96.

24. El-Rifai W, Moskaluk CA, Abdrabbo MK, et al. Gastric cancers overexpress S100A calcium-binding proteins. Cancer Res 2002;62:6823-6.

25. Beers R, Chowdhury P, Bigner D, Pastan I. Immunotoxins with increased activity against epidermal growth factor receptor vIII-expressing cells produced by antibody phage display. Clin Cancer Res 2000;6:2835-43.

26. Buchner J, Pastan I, Brinkmann U. A Method for Increasing the Yield of Properly Folded Recombinant Fusion Proteins: Single-Chain Immunotoxins from Renaturation of Bacterial Inclusion Bodies. Anal Biochem 1992;205:263-70.

27. Wikstrand CJ, Hale LP, Batra SK, et al. Monoclonal antibodies against EGFRvIII are tumor specific and react with breast and lung carcinomas and malignant gliomas. Cancer Res 1995;55:3140-8.

28. Sambrook J, Russell DW. Molecular cloning : a laboratory manual. 3rd / ed. Cold Spring Harbor, N.Y.: Cold Spring Harbor Laboratory Press; 2001.

29. Chu CT, Everiss KD, Wikstrand CJ, Batra SK, Kung HJ, Bigner DD. Receptor dimerization is not a factor in the signalling activity of a transforming variant epidermal growth factor receptor (EGFRvIII). Biochem J 1997;324:855-61.

30. Wikstrand CJ, McLendon RE, Friedman AH, Bigner DD. Cell surface localization and density of the tumor-associated variant of the epidermal growth factor receptor, EGFRvIII. Cancer Res 1997;57:4130-40.

31. Reist CJ, Archer GE, Kurpad SN, et al. Tumor-specific anti-epidermal growth factor receptor variant III monoclonal antibodies: use of the tyramine-cellobiose radioiodination method enhances cellular retention and uptake in tumor xenografts. Cancer Res 1995;55:4375-82.

32. Reist CJ, Archer GE, Wikstrand CJ, Bigner DD, Zalutsky MR. Improved targeting of an anti-epidermal growth factor receptor variant III monoclonal antibody in tumor xenografts after labeling using N-succinimidyl 5-iodo-3-pyridinecarboxylate. Cancer Res 1997;57:1510-5.

33. Lindmo T, Boven E, Cuttitta F, Fedorko J, Bunn P, Jr. Determination of the immunoreactive fraction of radiolabeled monoclonal antibodies by linear extrapolation to binding at infinite antigen excess. J Immunol Methods 1984;72:77-89.

34. Kuan CT, Wikstrand CJ, Archer G, et al. Increased binding affinity enhances targeting of glioma xenografts by EGFRvIII-specific scFv. Int J Cancer 2000;88:962-9.

35. Kleihues P, Burger PC, Scheithauer BW, Zülch KJ. Histological typing of tumours of the central nervous system. 2nd / ed. Berlin ; New York: Springer-Verlag; 1993.

36. Grant CE, Kurz EU, Cole SP, Deeley RG. Analysis of the intron-exon organization of the human multidrug-resistance protein gene (MRP) and alternative splicing of its mRNA. Genomics 1997;45:368-78.

37. Shapiro MB, Senapathy P. RNA splice junctions of different classes of eukaryotes: sequence statistics and functional implications in gene expression. Nucleic Acids Res 1987;15:7155-74.

38. Tsuka H, Mori H, Li B, Kanamaru H, Matsukawa S, Okada K. Expression of c-MET/HGF receptor mRNA and protein in human non-malignant and malignant prostate tissues. Int J Oncol 1998;13:927-34.

39. Capone PM, Papsidero LD, Chu TM. Relationship between antigen density and immunotherapeutic response elicited by monoclonal antibodies against solid tumors. J Natl Cancer Inst 1984;72:673-7.

40. Ahn JH, Lee Y, Jeon C, et al. Identification of the genes differentially expressed in human dendritic cell subsets by cDNA subtraction and microarray analysis. Blood 2002;100:1742-54.

41. Bobo RH, Laske DW, Akbasak A, Morrison PF, Dedrick RL, Oldfield EH. Convection-enhanced delivery of macromolecules in the brain. Proc Natl Acad Sci U S A 1994;91:2076-80.

42. Archer GE, Sampson JH, Lorimer IA, et al. Regional treatment of epidermal growth factor receptor vIII-expressing neoplastic meningitis with a single-chain immunotoxin, MR-1. Clin Cancer Res 1999;5:2646-52.

43. Ali-Osman F, Brunner JM, Kutluk TM, Hess K. Prognostic significance of glutathione S-transferase pi expression and subcellular localization in human gliomas. Clin Cancer Res 1997;3:2253-61.

44. Bhowmick DA, Zhuang Z, Wait SD, Weil RJ. A functional polymorphism in the EGF gene is found with increased frequency in glioblastoma multiforme patients and is associated with more aggressive disease. Cancer Res 2004;64:1220-3.

Exhibit 7.

Table 1. Incidence of *gpnmb* mRNA expression from newly diagnosed GBM patients

Diagnosis	Incidence	
	Positive[a]	> 10-fold[b]
Overall $gpnmb_{wt+sv}$ transcripts	35/50 (70%)	19/50 (38%)
$gpnmb_{wt}$ transcripts	26/50 (52%)	11/50 (22%)
Splice variant $gpnmb_{sv}$ transcripts	15/50 (30%)	3/50 (6%)

[a] Detected by real-time RT-PCR analysis; positive cases were defined as those with *gpnmb* RNA levels 3-fold higher than normal brain.

[b] More than 10-fold greater than normal whole brain sample

Exhibit 8

Table 2. Summary of immunohistochemical evaluation of frozen GBM tissue sections from newly diagnosed patients with polyvalent anti-GPNMB antiserum #2640 and/or MAb G11

Patterns	Positive cases/Total cases
anti-GPNMB staining*	52/79 (66%)
parenchymal staining	30/52 (58%)
Prominent perivascular staining	8/52 (15%)
Both parenchymal and perivascular staining	14/52 (27%)

*32 cases were stained concurrently with both antiserum #2640 and MAb G11; in 31/32 cases (97%) the result (+ or -) and staining pattern observed were completely concordant. There was a slight tendency for staining with MAb G11 to be more intense (Exhibit 4, panels C and I). The single discrepancy was a GBM sample positive with MAb G11, exhibiting a diffuse parenchymal pattern; it was negative with antiserum #2640.

Exhibit 9

Table 3. A. Univariate Cox model analyses of the relationship between patient survival and levels of *gpnmb* RNA and the presence of GPNMB protein by A. immunohistochemistry B. Kaplan Meier Survival Estimates C. Multivariate Cox models of the relationship between the levels of *gpnmb* RNA, presence of GPNMB protein by immunohistochemistry and patient survival

A.

Variable	Hazard Ratio	95% CI	p-value
Relative RNA_{sv+wt} Expression: > 3.0 vs. ≤ 3.0	3.0	(1.3 , 7.1)	0.013
Relative RNA_{wt} Expression: > 3.0 vs. ≤ 3.0	2.2	(1.1 , 4.5)	0.031
Relative RNA_{sv} Expression: > 3.0 vs. ≤ 3.0	1.4	(0.7 , 2.8)	0.406
Immunohistochemisty: Positive vs Zero	2.8	(1.2 , 6.3)	0.013

B.

Variables	N	Dead	2yr Survival Probability	95% CI	Median Survival (Weeks)	95% CI
RNAsv+wt ≤ 3.0	12	8	42%	(21% , 81%)	90.0	(44.9 , ∞)
RNAsv+wt > 3.0	27	27	15%	(6% , 37%)	55.1	(40.3 , 83.0)
RNAwt ≤ 3.0	20	16	35%	(19% , 64%)	61.6	(50.1 , ∞)
RNAwt > 3.0	19	19	11%	(3% , 39%)	53.4	(39.7 , 92.3)
RNAsv ≤ 3.0	28	24	25%	(13% , 48%)	54.9	(40.3 , 98.4)
RNAsv > 3.0	11	11	18%	(5% , 64%)	82.4	(49.9 , ∞)
Negative IHC	13	9	39%	(19% , 77%)	90.0	53.4 , ∞)
Positive IHC	26	26	15%	(6% , 38%)	50.1	(39.1 , 86.6)

C.

Variable	Hazard Ratio	95% CI	p-value
Age	1.1	(1.0, 1.1)	0.002
Relative RNA_{wt} Expression: > 3.0 vs. ≤ 3.0	2.6	(1.2, 5.5)	0.011

Variable	Hazard Ratio	95% CI	p-value
Age	1.0	(1.0, 1.1)	0.001
Immunohistochemisty: Positive vs Zero	2.6	(1.2, 5.9)	0.021